

Original Research

Calculation of Photons Reaction Rate Resulting at 120 kVp X-ray Tube Voltage and 1 mAs as Function to Digital Imaging and Communications in Medicine Pixel Numbers Using Monte Carlo N-Particle Transport and a Voxel Model of a 29-Year-Old Patient

Tawfik A. Shdeed, PhD*

2nd Faculty of Mechanical and Electrical Engineering, Damascus University, Syria

*Corresponding author

Tawfik A. Shdeed, PhD

2nd Faculty of Mechanical and Electrical Engineering, Damascus University, Syria; E-mail: ashdeedtaw@gmail.com

Article information

Received: August 8th, 2020; Accepted: September 15th, 2020; Published: October 27th, 2020

Cite this article

Shdeed TA. Calculation of photons reaction rate resulting at 120 kVp X-ray tube voltage and 1 mAs as function to digital imaging and communications in medicine pixel numbers using monte carlo N-particle transport and a voxel model of a 29-year-old patient. *Radiol Open J.* 2020; 4(2): 46-54. doi: [10.17140/ROJ-4-131](https://doi.org/10.17140/ROJ-4-131)

ABSTRACT

Purpose

To read the digital imaging and communications in medicine (DICOM) images of brain and extract intensity values and build a three dimensional model for Monte Carlo n-particle transport (MCNP) code input file in purpose to study the average particle flux and deposited energy of X-Ray photons resulting at 120 kVp and 1 mAs (form point source) as function to DICOM pixel numbers in the brain tissues for a 29-year-old female patient using MCNP code and Matlab program to read the DICOM images.

Method

The matrix laboratory (MATLAB) program was used to read the DICOM images and extract the intensity values in each pixel of the DICOM image corresponding to certain slice of the brain. These color levels are characteristic of different tissue, and have been relied upon to create the specific material in each volume element in MCNP input file.

Results

The percentage of tissues with computed tomography (CT) numbers less than 100 (except air between source and patient) equals to 87.11% and the sum of deposited energy over these regions equals to $1.77 \times 10^{10} \frac{\text{MeV}}{\text{g}}$, but the tissues with CT numbers greater than 100 equals to 12.89% and absorbed dose in these tissues reach to $9.12 \times 10^9 \frac{\text{MeV}}{\text{g}}$. Also the X-ray photon flux can be reach to $6.30 \times 10^{11} \frac{\text{p}}{\text{cm}^2 \cdot \text{s}}$ at surface of skin, and drops to $10^9 \frac{\text{p}}{\text{cm}^2 \cdot \text{s}}$ when passing the bones of the skull and skin where photons deposit most of their energy.

Conclusion

Values of the deposited energy at surface of skin are high, so it is always necessary to be cautious when performing the examination to obtain acceptable images from the first time and without having to repeat the imaging again for the same case unless there are necessities for it.

Keywords

Computed tomography (CT); X-ray; Voxel phantom; MCNP Code; Average particle flux; Matlab.

INTRODUCTION

Computed tomography (CT), contributes over 34% of collective dose from diagnostic X-rays examination in the world,¹

where the dose resulting from CT scanner (for whole body examination estimated at 10 mSv, while dose during conventional imaging estimated at 0.02-0.04 mSv), therefore the difference is very large between the two scans can be reach to 400-500 times.

Because these radiations is not visible, the resulting dangers do not appear directly, but have a stochastic effects that can appear in subsequent years or generations, It was therefore necessary to adjust and monitor the radiation doses resulting from these practices and to assess the radiation risks resulting from them. Table 1 gives a comparison between the effective dose resulting from the computed tomography and each of the traditional imaging of the chest and the number of years of exposure to natural background radiation which produces the same effective dose resulting from computed tomography.¹

Table 1. A Comparison between the Effective Dose Resulting from the Computed Tomography and Each of the Traditional Imaging of the Chest and the Number of Years of Exposure to Natural Background Radiation Which Produces the Same Effective Dose Resulting from Computed Tomography

Imaging Protocol	Effective Dose (mSv)	Number of the Chest's Images in the Traditional Imaging	Number of Years of Exposure to Natural Background Radiation
Head scan	2.3	115	1-year
Chest scan	8	400	3.6-year
abdomen and pelvis scan	10	500	4.5-year

According to some statistics, the number of computed tomography devices in Syria exceeds 232 devices, serving more than 19 million people, where one machine serves about 86 thousand people, therefore It is necessary to assess the effects of these devices on an ongoing basis.

Matlab Program

The matrix laboratory (MATLAB) platform is optimized for solving engineering and scientific problems. The matrix-based MATLAB language is the world's most natural way to express computational mathemati.² CT DICOM images were read using the MATLAB program in purpose to construct a three-dimensional phantom (voxels phantom), therefore, the following commands have been implemented, {DICOMINFO, DICOMREAD, IMSHOW, MIN, MAX, IMTOOL}.

Monte Carlo N-Particle Code

Monte Carlo n-particle code (MCNP) is a general-purpose MCNP that can be used for neutron, photon, electron, or coupled neutron/photon/electron transport, including the capability to calculate given values for critical systems. for photons, the code accounts for incoherent and coherent scattering, the possibility of fluorescent emission after photoelectric absorption, absorption in pair production with local emission of annihilation radiation, and bremsstrahlung.³

Purposes of the Research

To read the dicom images of brain and extract intensity values and build a three dimensional model for mcnp code input file in purpose to study the average particle flux and deposited energy of X-ray photons resulting at 120 kvp and 1 mas as function to DICOM pixel numbers in the brain tissues for a 29-year-old fe-

male patient using MCNP code and MATLAB program to read the DICOM images.

METHODS AND MATERIALS

The General CT Model

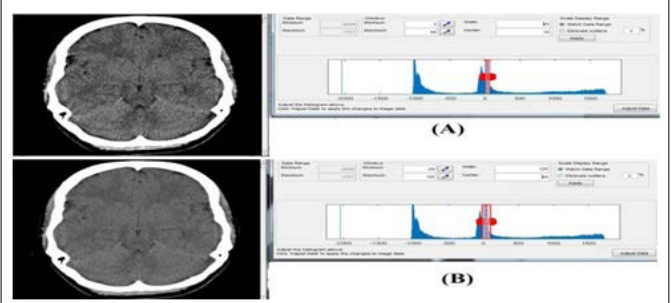
In this study was based on a ct scan of a female patient aged 29-years, using a scanner, the multislice helical ct scanner was used for all simulations. it is a third generation CT scanner quipped with solid state detectors system. Scan time for full helical scan is 100 seconds. The operating voltage are 80, 100, 120 and 135 kVp and the tube current can vary from 30 to 300 mAs in steps of 10 mAs. Table 2 shows the specifications of the CT images and the CT scanner used for this study.

Table 2. The Specifications of the CT Scan Device Used for This Study

Format: 'DICOM'	GeneratorPower: 26
FormatVersion: 3	CTDIvol: 83
Width: 512	PatientOrientation: 'LIP'
Height: 512	SamplesPerPixel: 1
BitDepth: 16	PhotometricInterpretation: 'MONOCHROME2'
ColorType: 'grayscale'	Rows: 512
ImplementationVersionName: 'DCMOBJ4.3.28.5'	Columns: 512
ImageType: 'ORIGINAL\PRIMARY\AXIAL'	WindowCenter: 40
AccessionNumber: '1611'	WindowWidth: 120
PatientSex: 'F'	TableHeight: 46
PatientAge: '029Y'	RotationDirection: 'CW'
BodyPartExamined: 'HEAD'	ExposureTime: 1500
ScanOptions: 'NORMAL_CT'	XrayTubeCurrent: 220
SliceThickness: 4	Exposure: 330
KVP: 120	ProtocolName: 'Brain S&S 4mm'

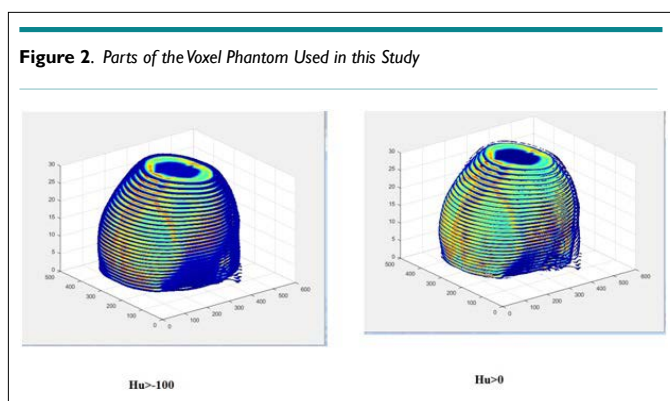
In order to get better contrast of the tissues, the following values were modified, the window's minimum intensity value=3, the window's maximum intensity value=68 that corresponding to window's width=65 and window's center=35 instead of window's width=120 and window's center=40. As shown in Figure 1.

Figure 1. Comparison between Two Cases of Window Intensity Vvalues, (A) The Window's Width=65 and Window's Center=35. (B) Window's Width=120 and Window's Center=40



Voxel Phantom

Figure 2 shows the voxel phantom that was adopted in this study of the head region. This phantom consists of a number of voxels (512×512×100) with voxel size 0.2×0.2×1 cm³, in this case each pixel will be corresponded to one voxel, i.e. each pixel will be represented within 0.2×0.2×1 cm³. Figure 2 shows parts of this phantom plotted for the entire digital image matrix (512×512). Parts of it were displayed because of the difficulty of showing the entire phantom according to the PC used in this study. Where used In this study a computer with (core i5- CPU 2.30 GHz processor) and 1 Gb VGA. On the Figure 2, the areas appear stretch from the blue color that corresponds to the least color intensity (the lowest values for the CT number, Hu=-950, that corresponding to the air material) and upto the red color (which corresponds to the highest values for the CT number, Hu=1370, that corresponding to the Skeleton cortical bone material).



Materials Assign

The CT images were read using the Matlab program, after that, the images were then resized to a scale of 325×171 pixel, in accordance with the number of identical voxels in the phantom used in the study. Firstly, in the input file of MCNP code, the equivalent substances were created for air, soft brain tissue, red blood cells, spinal cord, skin, facial and skull bones, Adipose tissue, Yellow marrow, Cell nucleus, Red marrow, lymph, eye lens,.. etc. secondly, each material was given a number and a universe number (U) that corresponding to certain range of CT numbers that defined each pixel in image. The values of the chemical composition and the CT numbers (in Hounsfield) and density were taken from several references such as.⁴⁻⁶ Table 3 shows chemical composition as percentages, density ρ and Hounsfield numbers for various tissue descriptions.

Source Modeling

In order to determine the energy spectrum of X-ray photons emitted at certain value of tube voltage (kVp), the X-ray tube was simulated using MCNP code. the energy spectrum of the photons produced was calculated at several voltage values, as shown in Figure 3. To calculate the average particle flux and deposited energy X-ray source was simulated as point source at distance from the center of phantom equals to 100 cm on X_{axis}, and variable step on Z_{axis} Figure 4 (1).

Average Particle Flux in a Cell and Deposited Energy

In this study we used the “F4” (cell fluence) tally to calculate reac-

Table 3. Chemical Composition as Percentages, Density ρ (taken from ICRP 1975) and Calculated. Hounsfield Numbers for Various Tissue Descriptions⁴⁻⁶

Tissue	Density [g/cm ³]	Fraction Weight %											CT Number	
		Fe	K	Cl	S	Mg	Na	P	Ca	O	N	C		H
Air	0.001294									23.2	75.3	0.01	0	<-950
Adipose tissue	0.95			0.1	0.1		0.1			27.8	0.7	59.8	11.4	-70
Red marrow	1.03	0.1	0.2	0.2	0.2			0.1		43.9	3.4	41.4	10.5	14
Lymph	1.03			0.4	0.1		0.3			83.2	1.1	4.1	10.8	28
Skin	1.09		0.1	0.3	0.2		0.2	0.1		64.5	4.2	20.4	10	75
Cartilage	1.1			0.3	0.9		0.5	2.2		74.4	2.2	9.9	9.6	98
Spongiosa	1.18	0.1	0.1	0.2	0.2	0.1	0.1	3.4	7.4	36.7	2.8	40.4	8.5	260
Skeleton-sacrum	1.29	0.1	0.1	0.1	0.2	0.1		4.5	9.8	43.8	3.7	30.2	7.4	413
Skeleton-vertebral column (D6, L3)	1.33	0.1	0.1	0.1	0.2	0.1		5.1	11.1	43.7	3.8	28.7	7	477
Skeleton-femur	1.33			0.1	0.2	0.1	0.1	5.5	12.9	36.8	2.8	34.5	7	499
Skeleton-ribs (2 nd , 6 th)	1.41		0.1	0.1	0.3	0.1	0.1	6	13.1	43.6	3.9	26.3	6.4	595
Skeleton-vertebral column (C4)	1.42	0.1	0.1	0.1	0.3	0.1	0.1	6.1	13.3	43.6	3.9	26.1	6.3	609
Skeleton-humerus	1.46				0.2	0.1	0.1	7	15.2	36.9	3.1	31.4	6	683
Skeleton-ribs (10 th)	1.52		0.1	0.1	0.3	0.1	0.1	7.2	15.6	43.4	4	23.5	5.6	763
Skeleton--cranium	1.61				0.3	0.2	0.1	8.1	17.6	43.5	4	21.2	5	903
Skeleton-mandible	1.68				0.3	0.2	0.1	8.6	18.7	43.5	4.1	19.9	4.6	1006
Skeleton--cortical bone	1.92				0.3	0.2	0.1	10.3	22.5	43.5	4.2	15.5	3.4	1376

tion rate across slice that gives a quantity in units of particle/cm² per source particle.³

The average particle flux in a cell can be written:

$$\bar{\Phi}_V = \frac{1}{V} \int dE \int dt \int dV \int d\Omega \Psi(\vec{r}, \hat{\Omega}, E, t) = \frac{1}{V} \int dE \int dV \int dt vN(\vec{r}, E, t)$$

Where: $N(\vec{r}, E, t) = \int d\Omega n(\vec{r}, \hat{\Omega}, E, t)$ is the density of particles.

Cell heating and energy deposition tallies are track length flux tallies modified totally a reaction rate convolved with an energy-dependent heating function, The units of the heating tally are

MeV/g, the heating number H(E) for photons is³:

$$H(E) = E - \sum_{i=1}^3 p_i(E) [\bar{E}_{i,out}(E)]$$

Where: i=1 incoherent (Compton) scattering with form factors, i=2 pair production;

$\bar{E}_{i,out}(E) = 2m_0c^2 = 1.022016$ MeV, i=3 photoelectric absorption $\bar{E}_{i,out}(E) = 0$ p_t(E): probability of reaction i at gamma incident energy E.

$\bar{E}_{i,out}(E)$ average exiting gamma energy for reaction i at photon incident energy E.

Figure 3. The Spectrum Energy of X-ray Photons Emitted at Several Values of Tube Voltage Calculated Using the MCNP Code

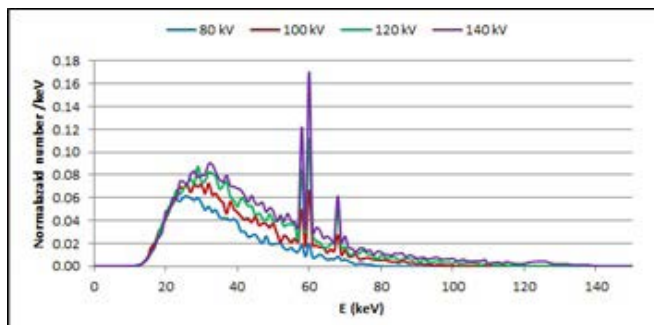


Figure 4 (1). The X-ray Point Source Modeling, X-ray Photons Distribution Using MCNP Code

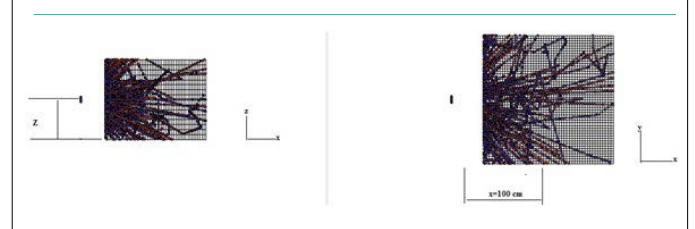


Table 4. The Average of Deposited Energy, Mean Free Path and Mss Attenuation Coefficient as Function to CT Numbers for 33 Slice in CT DICOM Images of Head

CT Number Range		Deposited Energy [MeV/g/ImAs]	Mean free path mfp (cm)	$\frac{\mu}{\rho}$ cm ² /g	CT Number		Deposited Energy [MeV/g/ImAs]	Mean free path mfp (cm)	$\frac{\mu}{\rho}$ cm ² /g
From	To				From	To			
-2084	-741	3.90E+11	2829.10	0.32	53	54	2.92E+07	3.87	0.24
-741	-70	4.83E+09	3.96	0.26	54	55	3.44E+07	3.94	0.23
-70	-42	2.17E+09	4.33	0.24	55	60	1.34E+08	3.95	0.23
-42	2	4.20E+09	3.92	0.25	60	75	2.56E+08	4.12	0.23
2	3	9.94E+07	3.78	0.26	75	100	2.78E+08	3.85	0.24
3	14	5.13E+08	3.91	0.23	100	260	1.36E+09	2.93	0.29
14	28	2.83E+09	4.52	0.22	260	270	3.47E+07	3.02	0.28
28	31	6.09E+08	4.48	0.22	270	413	7.36E+08	2.51	0.30
31	32	1.89E+08	4.44	0.22	413	477	2.52E+08	2.56	0.30
32	37	6.64E+08	4.36	0.23	477	499	4.90E+07	2.25	0.32
37	40	2.80E+08	3.91	0.24	499	595	3.44E+08	2.28	0.31
40	42	1.22E+08	4.04	0.23	595	609	9.78E+07	2.26	0.31
42	43	5.39E+07	4.05	0.24	609	683	3.52E+08	2.06	0.32
43	44	4.81E+07	16.35	0.23	683	763	2.42E+08	1.95	0.32
44	45	5.42E+07	4.00	0.23	763	903	5.92E+08	1.87	0.33
45	50	1.99E+08	3.92	0.24	903	1006	5.93E+08	1.91	0.32
50	53	1.02E+08	4.05	0.23	1006	2400	4.47E+09	1.59	0.33

RESULTS

As have been explained previously, all calculations were done for point source at 1 mAs and 120 kVp and 4 mm slice thickness. Table 4 shows the average of deposited energy in (MeV/g/1mAs), mean free path, and mass attenuation coefficient as function to CT numbers for 33 slice of head Figure 4 (2).

Since CT_Number in Hounsfield units HU is given by:

$$HU = 1000 \frac{\mu - \mu_w}{\mu_w}$$

Therefore At low energies (<15 keV), the photoelectric effect accounts for virtually all of the interactions in water. As the photon energy increases photoelectric coefficient drops rapidly and Compton scattering interactions become dominant in water at about 100 keV. Figure 5 shows a plot of average particle flux (red curve) and deposited energy (blue curve) resulting from X-ray photons at 1 mAs current intensity as function to pixel numbers on x axis for several slices of head.

The number of radiation pulses that enter and/or traverse a medium is governed by inverse square law, which states that the flux of radiation emitted from a point source is inversely proportional to r^2 , at the beginning of tissues (pixel's number 100) most of X ray photons will be absorbed in the skin and skeleton—cranium bone because the value of total attenuation coefficient generally increase as the Z of the medium increases. where photoelectric interactions are increased in high-Z materials especially for low-energy photons.

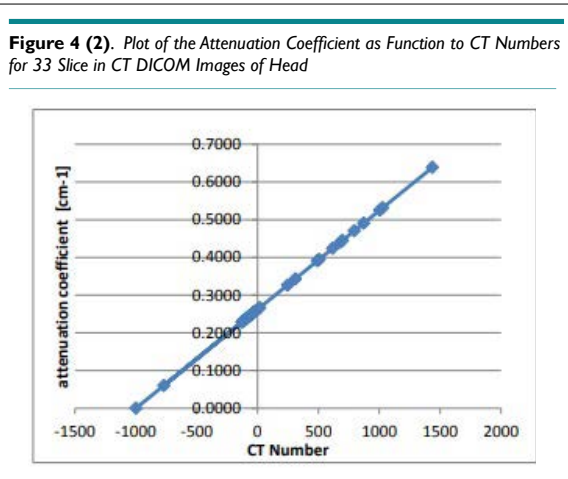


Figure 4 (2). Plot of the Attenuation Coefficient as Function to CT Numbers for 33 Slice in CT DICOM Images of Head

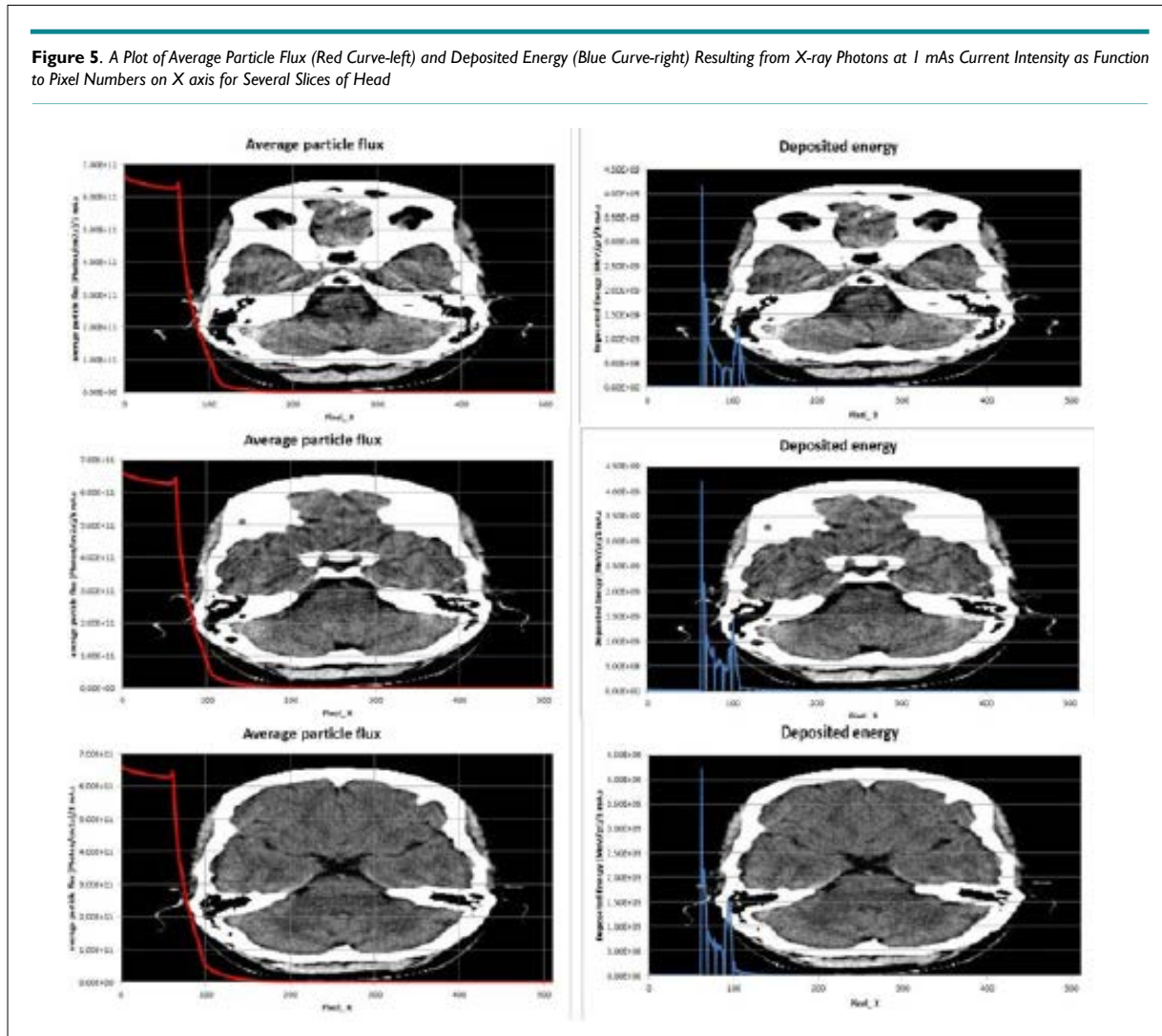
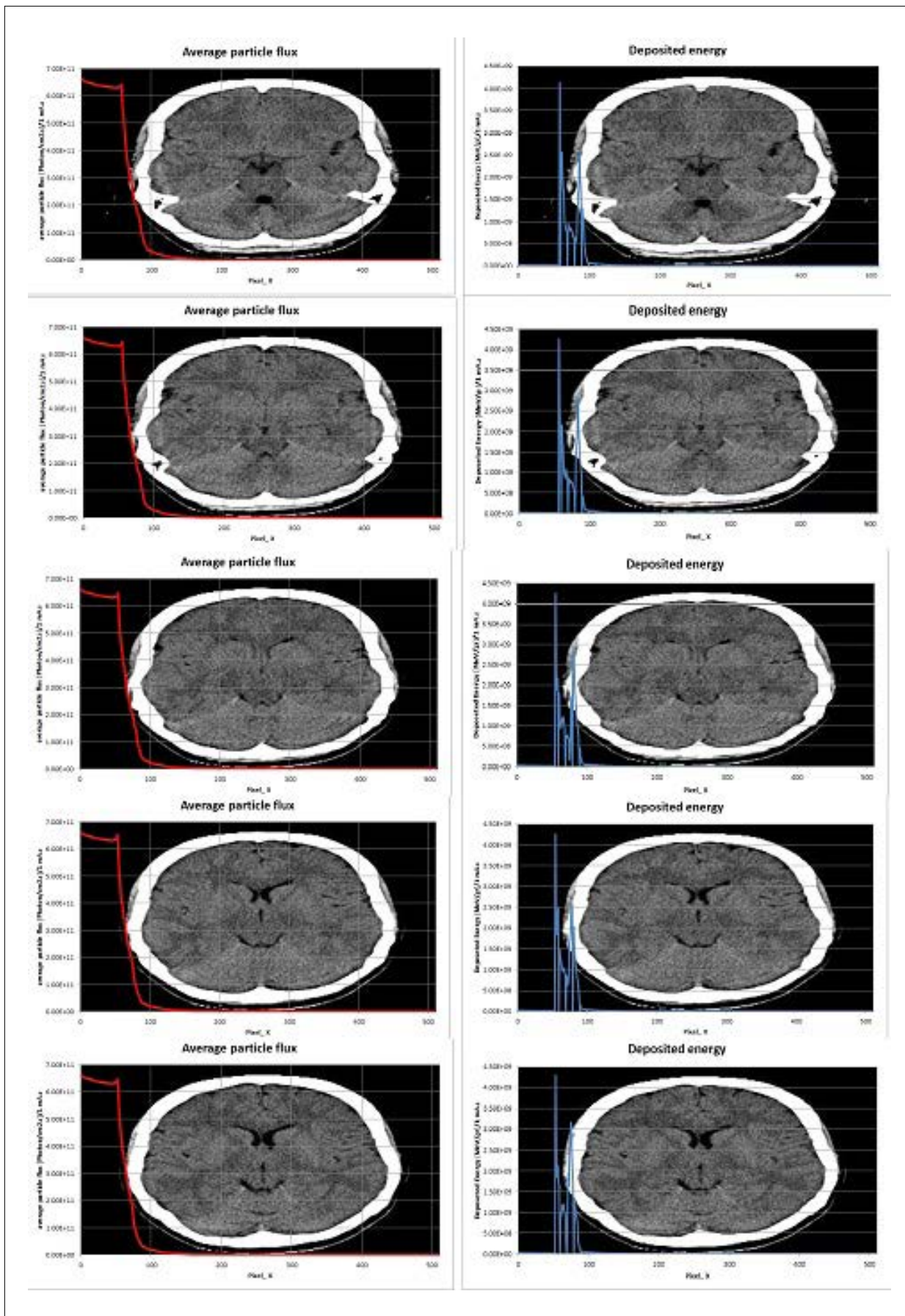


Figure 5. A Plot of Average Particle Flux (Red Curve-left) and Deposited Energy (Blue Curve-right) Resulting from X-ray Photons at 1 mAs Current Intensity as Function to Pixel Numbers on X axis for Several Slices of Head



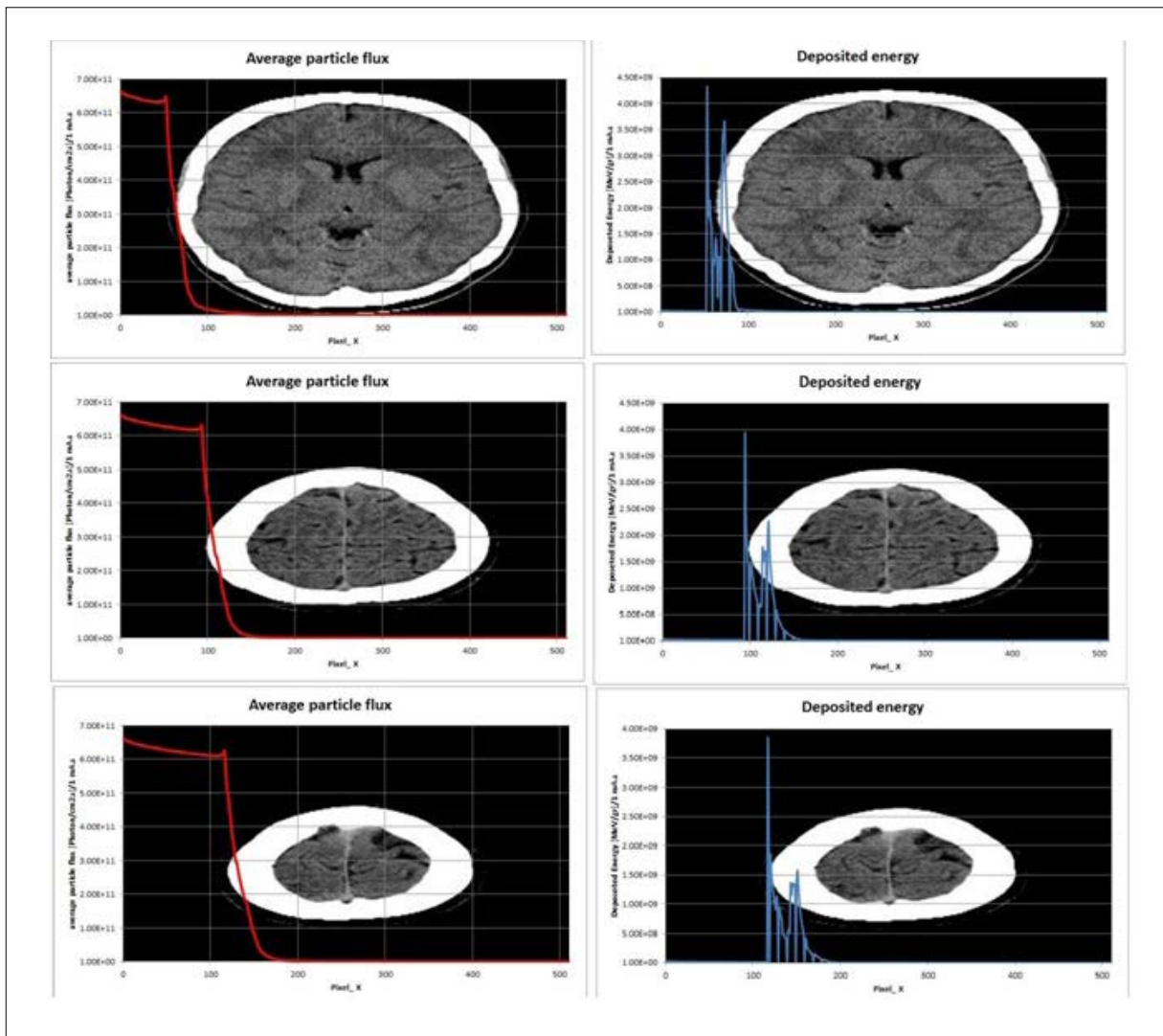
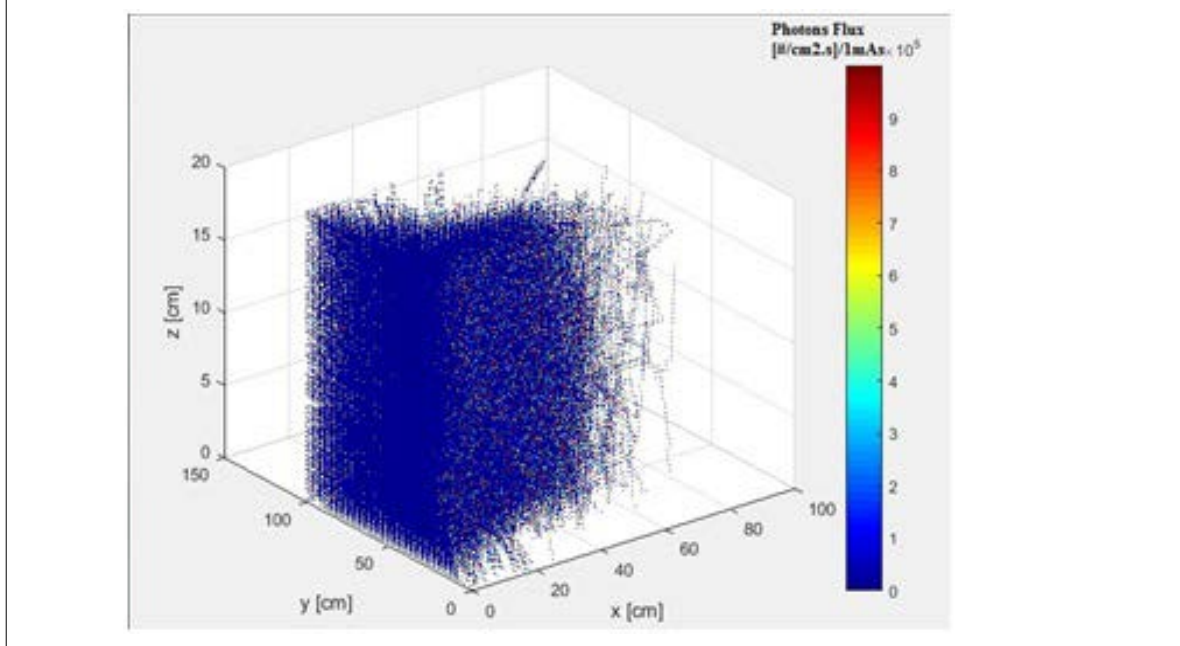


Figure 6. A Three-Dimensional Plot Representation of Photons Flux in the Phantom, When the Point Source of X ray Photons at $z=10$ cm (Middle of Scan Length)



While Figure 6 shows the distribution of photons flux in the phantom, when the point source of X ray photons at z=10 cm (middle of scan length).

DISCUSSION

In this research, we tried to use the available software to extrapolate and estimate the average particle flux, deposited energy, and mass attenuation coefficient depending on determine the mean free path of X-ray photons resulting at 120 kVp and 1 mAs as function to digital imaging and communications in medicine (DICOM) pixel numbers in the brain tissues for a 29-year-old female patient using MCNP code. Table 4 shows the change of deposited energy in (MeV/g /1mAs), mean free path (cm), and mass attenuation coefficient (cm²/g) as function to CT numbers of head CT images, these values can vary from one region to another according to CT numbers and their distribution and availability in each region, for example the abdominal region will contain the imaging numbers that represent the soft tissue at a higher rate than those representing the bones and cartilage. In this case (head scan images) the percentage of tissues with CT numbers less than 100 (except air between source and patient) equals to 87.11% and the sum of deposited energy over these regions equals to $1.77 \times 10^{10} \left(\frac{\text{MeV}}{\text{g}} \right) \frac{1}{1\text{mAs}}$, but the tissues with CT numbers greater than 100 equals to 12.89% and absorbed dose in these tissues reach to $9.12 \times 10^9 \left(\frac{\text{MeV}}{\text{g}} \right) \frac{1}{1\text{mAs}}$. From Figure 5 X-ray photon flux can be reach to $6.30 \times 10^{11} \left(\frac{\text{p}}{\text{cm}^2\text{s}} \right) \frac{1}{1\text{mAs}}$ at surface skin, this flux follows the inverse square law and drops to $10^9 \left(\frac{\text{p}}{\text{cm}^2\text{s}} \right) \frac{1}{1\text{mAs}}$ when passing the bones of the skull and skin where photons deposit most of their energy as shown in Figure 5.

osited energy over these regions equals to $1.77 \times 10^{10} \left(\frac{\text{MeV}}{\text{g}} \right) \frac{1}{1\text{mAs}}$, but the tissues with CT numbers greater than 100 equals to 12.89% and absorbed dose in these tissues reach to $9.12 \times 10^9 \left(\frac{\text{MeV}}{\text{g}} \right) \frac{1}{1\text{mAs}}$. From Figure 5 X-ray photon flux can be reach to $6.30 \times 10^{11} \left(\frac{\text{p}}{\text{cm}^2\text{s}} \right) \frac{1}{1\text{mAs}}$ at surface skin, this flux follows the inverse square law and drops to $10^9 \left(\frac{\text{p}}{\text{cm}^2\text{s}} \right) \frac{1}{1\text{mAs}}$ when passing the bones of the skull and skin where photons deposit most of their energy as shown in Figure 5.

From Figure 5 X-ray photon flux can be reach to $6.30 \times 10^{11} \left(\frac{\text{p}}{\text{cm}^2\text{s}} \right) \frac{1}{1\text{mAs}}$ at surface skin, this flux follows the inverse square law and drops to $10^9 \left(\frac{\text{p}}{\text{cm}^2\text{s}} \right) \frac{1}{1\text{mAs}}$ when passing the bones of the skull and skin where photons deposit most of their energy as shown in Figure 5.

when passing the bones of the skull and skin where photons deposit most of their energy as shown in Figure 5.

The Comparison

In order to validate the results obtained, these results were compared with a number of reference studies. Figure 7 shows a comparison between a plot of the energy spectrum of the X-ray photons calculated in this study at different voltage values and using

an aluminum filter with thickness (1.2 mm) and a tungsten rotating anode with angle of 12°, with those of the reference.⁷

Also, the effective dose calculated in this study was compared to the head region with those in the reference.⁸ The Table 5 shows the result of the comparison. Taking into account the weighting factor for tissue of the brain is 0.01 [ICRP 2007] and for bone and cartilage tissues is 0.01.

Reference No	Procedure	Approximate Effective Radiation Dose
8	Computed Tomography (CT)–Head	2 mSv
	Computed Tomography (CT)–Head, repeated	4 mSv
This study	with and without contrast material	3.97 Sv

CONCLUSION

The DICOM images of brain were read and the intensity values were extracted and organized within 7864320x4 double matrix in order to build a three dimensional model for MCNP code input file in purpose to study of absorbed dose in the brain tissues for a 29-year-old female patient during CT scan of the head at specific voltage and current of X-ray tube using MCNP code and Matlab program. The Matlab program was used to read the DICOM images and extract the intensity values in each pixel of the image corresponding to certain slice of the brain. These color levels are characteristic of different tissue, and have been relied upon to create the specific material in each volume element in MCNP input file. As a result the absorbed dose in soft tissues with CT numbers less than 98 (which the percentage is 87.11%) can be reach to 0.222 Gy/1mAs, and for tissues with CT numbers greater than 98 (which the percentage is 12.89%) can be reach to 0.174 Gy/1mAs. These values for the dose are high, so it is always necessary to be cautious when performing the examination to obtain acceptable images from the first time and without having to repeat the imaging again for the same case unless there are necessities for it.

REFERENCES

1. Kharita MH, Wali Kh Patient management practice in computed

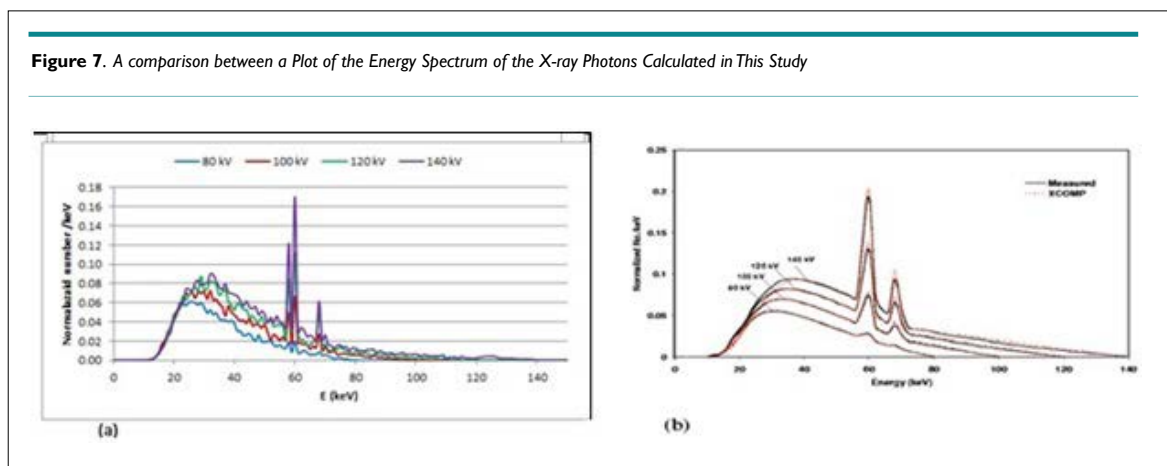


Figure 7. A comparison between a Plot of the Energy Spectrum of the X-ray Photons Calculated in This Study

- tomography with special emphasis to pediatric patients. Web site osti. <https://www.osti.gov/etdweb/biblio/21499832>. Accessed May 19, 2019.
2. The MathWorks. The Mathworks Website mathworks. <http://www.mathworks.com>. Accessed April 2, 2019.
 3. Mckinney G. *MCNP — A General Monte Carlo N-particle Transport Code, Version 5. X-5 Monte Carlo Team*. LA, USA: Los Alamos National Laboratory; 2003: 484.
 4. Schneider U, Pedron E, Lomax A. The calibration of CT Hounsfield units for radiotherapy treatment planning. *Physics in Medicine and Biology*. 1996; 41(1): 111-124. doi: 10.1088/0031-9155/41/1/009
 5. Massicano F, Massicano AVF, da Silv NG, Cintra FB, de Carvalho RM, Yoriyaz H. Analysis of CT and PET/SPECT images for dosimetry calculation. Paper presented at: International Nuclear Atlantic Conference; 2009; São Paulo, SP - Brazil.
 6. ASTAR and PSTAR databases. Web site physics.nist. <https://physics.nist.gov/cgi-bin/Star/compos.pl?matno=201>. Accessed May 19, 2019.
 7. M R Ay 1, S Sarkar, M Shahriari, D Sardari, H Zaidi. Assessment of different computational models for generation of X-ray spectra in diagnostic radiology and mammography. *Med Phys*. 2005; 32(6): 1660-1675. doi: 10.1118/1.1906126
 8. Radiological Society of North America (RSNA). Radiation Dose in X-Ray and CT Exams. Web site radiologyinfo. <http://www.radiologyinfo.org>. Accessed May 25, 2019.